EXHIBIT A

Submitted with Response to Office Action

dated December 28, 2005

MODERN COMPRESSIBLE FLOW

With Historical Perspective

Second Edition

John D. Anderson, Jr.

Professor of Aerospace Engineering
University of Maryland, College Park

McGraw-Hill Publishing Company

New York St. Louis San Francisco Auckland Bogotá Caracas
Hamburg Lisbon London Madrid Mexico Milan Montreal
New Delhi Oklahoma City Paris San Juan São Paulo
Singapore Sydney Tokyo Toronto

This book was set in Times Roman by Science Typographers, Inc.
The editors were Lyn Beamesderfer and John M. Morriss;
the production supervisor was Janelle S. Travers.
The cover was designed by Carla Bauer.
Project supervision was done by Science Typographers, Inc.
R. R. Donnelley & Sons Company was printer and binder.

MODERN COMPRESSIBLE FLOW
With Historical Perspective

234567890 DOC DOC 943210

ISBN 0-07-001673-9

Library of Congress Cataloging-in-Publication Data

Anderson, John David.
Modern compressible flow: with historical perspective / John D. Anderson, Jr.—2nd ed.
p. cm.—(McGraw-Hill series in aeronautical and aerospace engineering)
Includes index.
ISBN 0-07-001673-9
1. Fluid dynamics. 2. Gas dynamics. I. Title. II. Series.
QA911.A6 1990
629.132'323—dc20 89-12442

Chapter 5 - P163. FIRST MENTION OF CONTOUR

supersonic flow enters a diffuser, where it is slowed down in a convergent
sonic flow at the second throat, and then further slowed to low subsonic sp
a divergent duct, finally being exhausted to the atmosphere. This disc
along with Fig. 5.6, is a simplistic view of real supersonic wind tunnels
serves to illustrate the basic phenomena as revealed by the area-velocity r
Eq. (5.15). Also note that a convergent-divergent nozzle is sometimes c
de Laval (or *Laval*) *nozzle*, after Carl G. P. de Laval, who first used
configuration in his steam turbines in the late nineteenth century, as descr
Secs. 1.1 and 5.8.

The derivation of Eq. (5.15) utilized only the basic conservation eq
—no assumption as to the type of gas was made. Hence, Eq. (5.15) is a
relation which holds for real gases and chemically reacting gases, as well a
perfect gas—as long as the flow is isentropic. We will visit this matter a
Chap. 17.

5.4 ISENTROPIC FLOW OF A CALORICALLY PERFECT GAS THROUGH VARIABLE-AREA DUCTS

The analysis of flow through variable-area ducts in a general sense r
numerical solutions such as those to be discussed in Chap. 17. However, ba
our experience obtained in Chaps. 3 and 4, we suspect (correctly) that
obtain closed-form results for the case of a calorically perfect gas.

For example, consider the duct shown in Fig. 5.7. At the throat, the
sonic. Hence, denoting conditions at sonic speed by an asterisk, we have,
throat, $M^* = 1$ and $u^* = a^*$. The area of the throat is A^*. At any other
of the duct, the local area, Mach number, and velocity are A, M,
respectively. Apply Eq. (5.1) between these two locations:

$$\rho^* u^* A^* = \rho u A$$

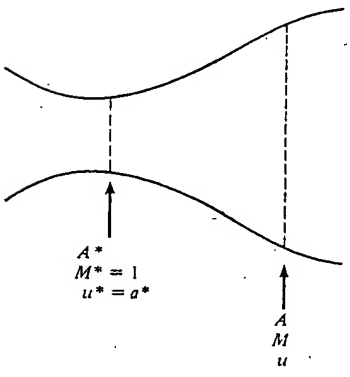

FIGURE 5.7
Geometry for derivation of the area Mach number

Since $u^* = a^*$, Eq. (5.16) becomes

$$\frac{A}{A^*} = \frac{\rho^*}{\rho}\frac{a^*}{u} = \frac{\rho^*}{\rho_o}\frac{\rho_o}{\rho}\frac{a^*}{u} \tag{5.17}$$

where ρ_o is the stagnation density defined in Sec. 3.4, and is constant throughout the isentropic flow. Repeating Eq. (3.31),

$$\frac{\rho_o}{\rho} = \left(1 + \frac{\gamma - 1}{2}M^2\right)^{1/(\gamma-1)}$$

and apply this to sonic conditions, we have

$$\frac{\rho_o}{\rho^*} = \left(\frac{\gamma + 1}{2}\right)^{1/(\gamma-1)} \tag{5.18}$$

Also, by definition, and from Eq. (3.37),

$$\left(\frac{u}{a^*}\right)^2 = M^{*2} = \frac{\dfrac{\gamma + 1}{2}M^2}{1 + \dfrac{\gamma - 1}{2}M^2} \tag{5.19}$$

Squaring Eq. (5.17), and substituting Eqs. (3.31), (5.18), and (5.19), we have

$$\left(\frac{A}{A^*}\right)^2 = \left(\frac{\rho^*}{\rho_o}\right)^2\left(\frac{\rho_o}{\rho}\right)^2\left(\frac{a^*}{u}\right)^2$$

$$\left(\frac{A}{A^*}\right)^2 = \left(\frac{2}{\gamma + 1}\right)^{2/(\gamma-1)}\left(1 + \frac{\gamma - 1}{2}M^2\right)^{2/(\gamma-1)}\left(\frac{1 + \dfrac{\gamma - 1}{2}M^2}{\dfrac{\gamma + 1}{2}M^2}\right)$$

$$\boxed{\left(\frac{A}{A^*}\right)^2 = \frac{1}{M^2}\left[\frac{2}{\gamma + 1}\left(1 + \frac{\gamma - 1}{2}M^2\right)\right]^{(\gamma+1)/(\gamma-1)}} \tag{5.20}$$

Equation (5.20) is called the *area Mach number relation*, and it contains a striking result. Turned inside out, Eq. (5.20) tells us that $M = f(A/A^*)$, i.e., the Mach number at any location in the duct is a function of the *ratio* of the local duct area to the sonic throat area. As seen from Eq. (5.15), A must be greater than or at least equal to A^*; the case where $A < A^*$ is physically not possible in an isentropic flow. Also, from Eq. (5.20) there are two values of M which correspond to a given $A/A^* > 1$, a subsonic and a supersonic value. The solution of Eq. (5.20) is plotted in Fig. 5.8, which clearly delineates the subsonic and supersonic branches. Values of A/A^* as a function of M are tabulated in Table A.1 for both subsonic and supersonic flow. For a given A/A^*, whether subsonic

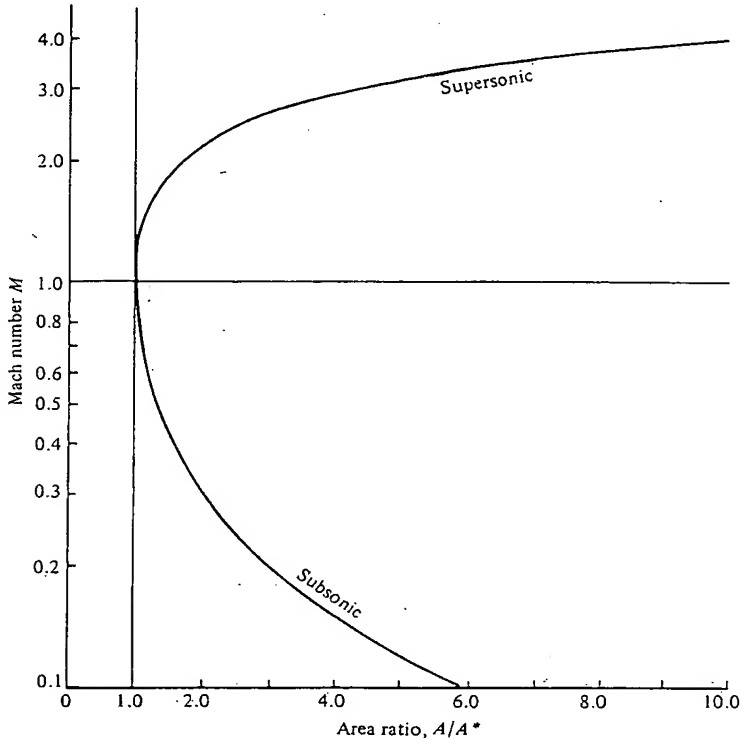

FIGURE 5.8
Area Mach number relation.

or supersonic flow exists depends on the boundary conditions, as desc
below.

Consider a given convergent-divergent nozzle, as sketched in Fig.
Assume that the area ratio at the inlet A_i/A^* is very large, $A_i/A^* \to \infty$, an
the inlet is fed with gas from a large reservoir at pressure and temperature p
T_o, respectively. Because of the large inlet area ratio, $M \approx 0$; hence p_o and
essentially stagnation (or total) values. Furthermore, assume that the
convergent-divergent nozzle expands the flow isentropically to supersonic s
at the exit. For the given nozzle, there is only *one* possible isentropic solutic
supersonic flow, and Eq. (5.20) is the key to this solution. In the conve
portion of the nozzle, the subsonic flow is accelerated, with the subsonic val
M dictated by the local value of A/A^* as given by the lower branch of Fig
The consequent variation of Mach number with distance x along the noz
sketched in Fig 5.9*b*. At the throat, where the throat area $A_t = A^*$, $M = 1$. I
divergent portion of the nozzle, the flow expands supersonically, witl
supersonic value of M dictated by the local value of A/A^* as given by the

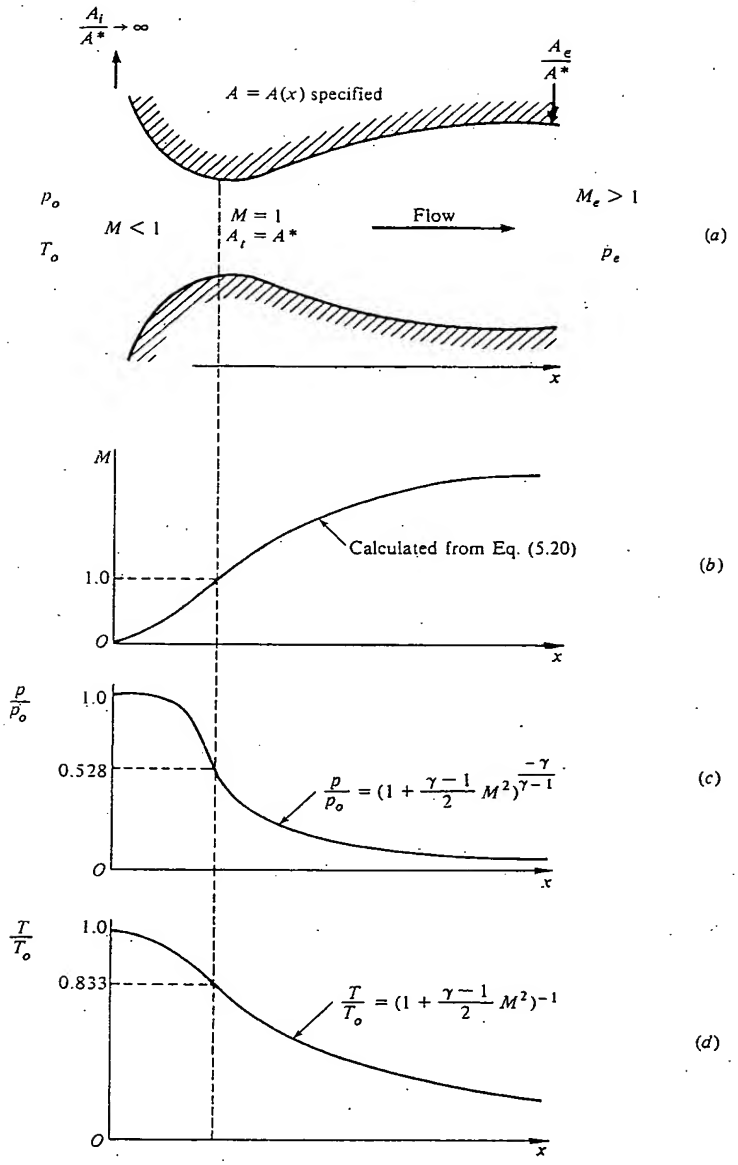

FIGURE 5.9
Isentropic supersonic nozzle flow.

branch of Fig. 5.8. This variation of M with x in the divergent nozzle is also sketched in Fig. 5.9*b*. Once the variation of Mach number through the nozzle is known, the variations of static temperature, pressure, and density follow from Eqs. (3.28), (3.30), and (3.31), respectively. The resulting variations of p and T are shown in Fig. 5.9*c* and *d*, respectively. Note that the pressure, density, and temperature decrease continuously throughout the nozzle. Also note that the exit pressure, density, and temperature ratios, p_e/p_o, ρ_e/ρ_o, and T_e/T_o depend only on the exit area ratio, A_e/A^* via Eq. (5.20). If the nozzle is part of a supersonic wind tunnel, then the test section conditions are completely determined by A_e/A^* (a geometrical design condition) and p_o and T_o (gas properties in the reservoir).

If a convergent-divergent nozzle is simply placed on a table, and nothing else is done, obviously nothing is going to happen; the air is not going to start rushing through the nozzle of its own record. To accelerate a gas, a pressure difference must be exerted, as clearly stated by Euler's equation, Eq. (5.9). Therefore, in order to establish a flow through any duct, the exit pressure must be lower than the inlet pressure, i.e., $p_e/p_0 < 1$. Indeed, for completely shockfree isentropic supersonic flow to exist in the nozzle of Fig. 5.9*a*, the exit pressure ratio must be precisely the value of p_e/p_o shown in Fig. 5.9*c*.

What happens when p_e/p_o is *not* the precise value as dictated by Fig. 5.9*c*? In other words, what happens when the backpressure downstream of the nozzle exit is independently governed (say by exhausting into an infinite reservoir with controllable pressure)? Consider a convergent-divergent nozzle as sketched in Fig. 5.10*a*. Assume that no flow exists in the nozzle, hence $p_e = p_o$. Now assume that p_e is minutely reduced below p_o. This small pressure difference will cause a small wind to blow through the duct at low subsonic speeds. The local Mach number will increase slightly through the convergent portion of the nozzle, reaching a maximum at the throat, as shown by curve 1 of Fig. 5.10*b*. This maximum will *not* be sonic; indeed it will be a low subsonic value. Keep in mind that the value A^* defined earlier is the *sonic* throat area, i.e., that area where $M = 1$. In the case we are now considering, where $M < 1$ at the minimum-area section of the duct, the real throat area of the duct, A_t, is larger than A^*, which for completely subsonic flow takes on the character of a reference quantity different from the actual geometric throat area. Downstream of the throat, the subsonic flow encounters a diverging duct, and hence M decreases as shown in Fig. 5.10*b*. The corresponding variation of static pressure is given by curve 1 in Fig. 5.10*c*. Now assume p_e is further reduced. This stronger pressure ratio between the inlet and exit will now accelerate the flow more, and the variations of subsonic Mach number and static pressure through the duct will be larger, as indicated by curve 2 in Fig. 5.10*b* and *c*. If p_e is further reduced, there will be some value of p_e at which the flow will just barely go sonic at the throat, as given by the curve 3 in Fig. 5.10*b* and *c*. In this case, $A_t = A^*$. Note that all the cases sketched in Fig. 5.10*b* and *c* are subsonic flows. Hence, for *subsonic* flow through the convergent-divergent nozzle shown in Fig. 5.10*a*, there are an *infinite number of isentropic solutions*, where both p_e/p_o and A/A_t are the controlling factors for the local flow properties at any given section. This is a direct contrast with the

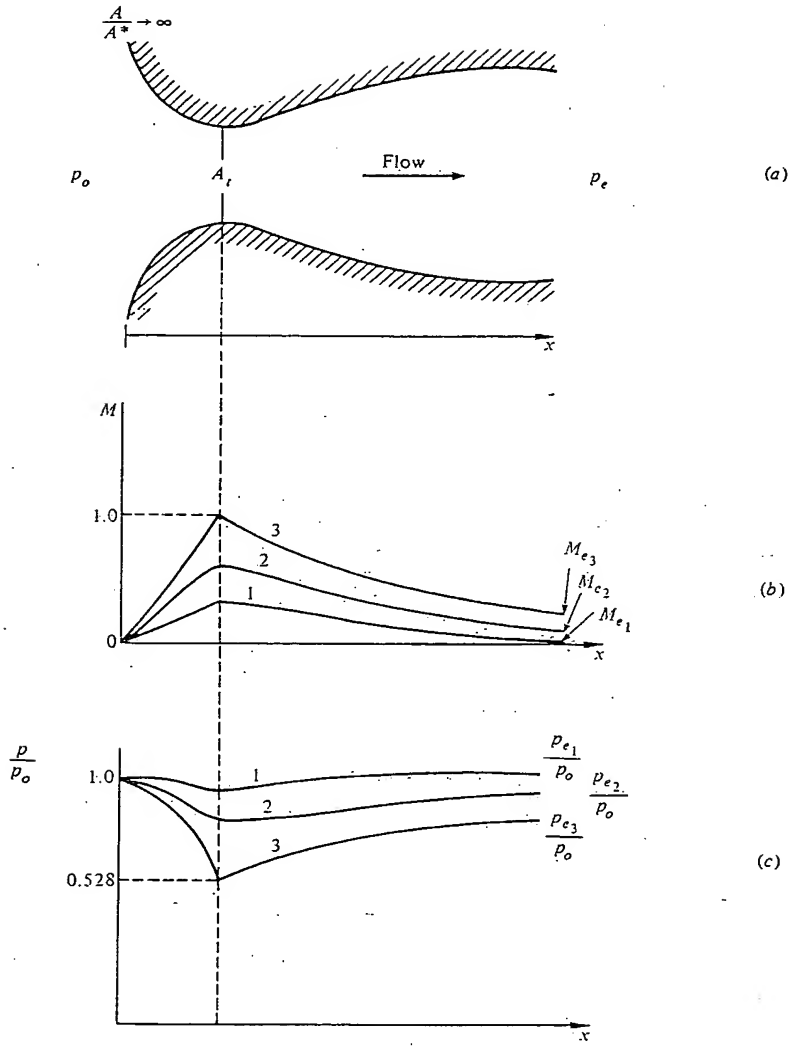

FIGURE 5.10
Subsonic flow in a convergent-divergent nozzle.

supersonic case discussed earlier, where only *one* isentropic solution exists for a given duct, and where A/A^* becomes the only controlling factor for the local flow properties (relative to reservoir properties).

For the cases shown in Fig. 5.10*a*, *b*, and *c*, the mass flow through the duct increases as p_e decreases. This mass flow can be calculated by evaluating Eq. (5.1) at the throat, $\dot{m} = \rho_t A_t u_t$. When p_e is reduced to p_{e_3}, where sonic flow is

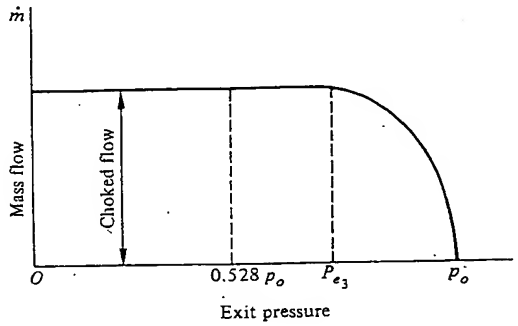

FIGURE 5.11
Variation of mass flow with exit pressure; illustration of choked flow.

attained at the throat, then $\dot{m} = \rho^* A^* a^*$. If p_e is now reduced further, $p_e < p_{e_3}$, the Mach number at the throat cannot increase beyond $M = 1$; this is dictated by Eq. (5.15). Hence, the flow properties at the throat, and indeed throughout the entire subsonic section of the duct, become "frozen" when $p_e < p_{e_3}$, i.e., the subsonic flow becomes unaffected and the mass flow remains constant for $p_e < p_{e_3}$. This condition, after sonic flow is attained at the throat, is called *choked flow*. No matter how low p_e is made, after the flow becomes choked, the mass flow remains constant. This phenomenon is illustrated in Fig. 5.11. Note from Eq. (3.35) that sonic flow at the throat corresponds to a pressure ratio $p^*/p_o = 0.528$ for $\gamma = 1.4$; however, because of the divergent duct downstream of the throat, the value of p_{e_3}/p_o required to attain sonic flow at the throat is larger than 0.528, as shown in Figs. 5.10*c* and 5.11.

What happens in the duct when p_e is reduced below p_{e_3}? In the convergent portion, as we stated above, nothing happens. The flow properties remain as given by the subsonic portion of curve 3 in Fig. 5.10*b* and *c*. However, a lot happens in the divergent portion of the duct. No isentropic solution is allowed in the divergent duct until p_e is adequately reduced to the specified low value dictated by Fig. 5.9*c*. For values of exit pressure above this, but below p_{e_3}, a normal shock wave exists inside the divergent duct. This situation is sketched in Fig. 5.12. Let the exit pressure be given by p_{e_4}. There is a region of supersonic flow ahead of the shock. Behind the shock, the flow is subsonic, hence the Mach number decreases towards the exit and the static pressure increases to p_{e_4} at the exit. The location of the normal shock wave in the duct is determined by the requirement that the increase of static pressure across the wave plus that in the divergent portion of the subsonic flow behind the shock be just right to achieve p_{e_4} at the exit. As the exit pressure is reduced further, the normal shock wave will move downstream, closer to the nozzle exit. It will stand precisely at the exit when $p_e = p_{e_5}$, where p_{e_5} is the static pressure behind a normal shock at the design Mach number of the nozzle. This is illustrated in Fig. 5.13*a*, *b*, and *c*. In Fig. 5.13*c*, p_{e_6} represents the proper isentropic value for the design exit Mach number. When the downstream backpressure p_B is further decreased such that

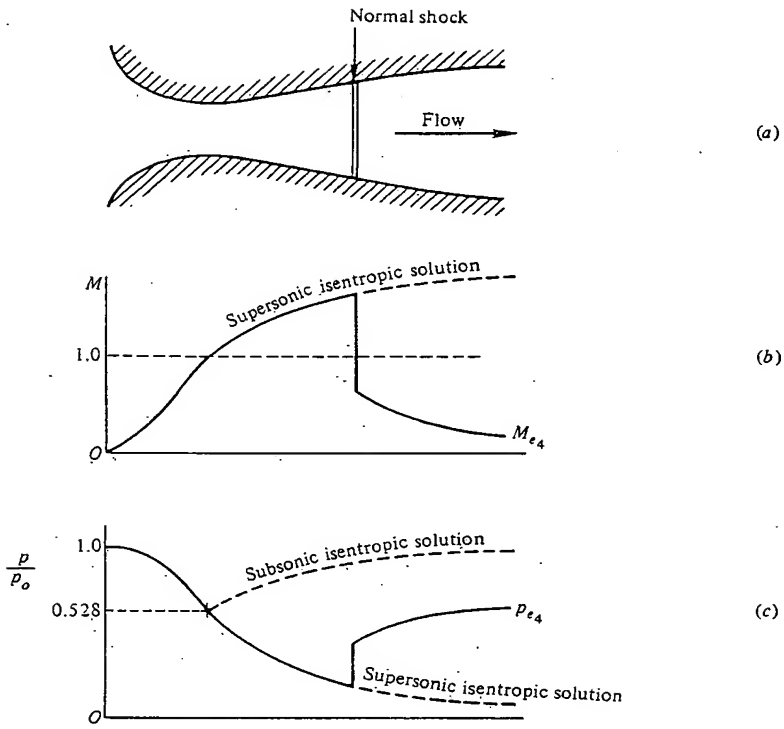

FIGURE 5.12
Flow with a shock wave inside a convergent-divergent nozzle.

$p_{e_6} < p_B < p_{e_5}$, the flow inside the nozzle is fully supersonic and isentropic, with the behavior the same as given earlier in Fig. 5.9*a*, *b*, *c*, and *d*. The increase to the backpressure takes place across an oblique shock attached to the nozzle exit, but outside the duct itself. This is sketched in Fig. 5.13*d*. If the backpressure is further reduced below p_{e_6}, equilibration of the flow takes place across expansion waves outside the duct, as shown in Fig. 5.13*e*.

When the situation in Fig. 5.13*d* exists, the nozzle is said to be *overexpanded*, because the pressure at the exit has expanded below the back pressure, $p_{e_6} < p_B$. Conversely, when the situation in Fig. 5.13*e* exists, the nozzle is said to be *underexpanded*, because the exit pressure is higher than the back pressure, $p_{e_6} > p_B$, and hence the flow is capable of additional expansion after leaving the nozzle.

The results of this section are particularly important and useful. The reader should make certain to reread this section until he or she feels comfortable with the concepts and results before proceeding further. Also, keep in mind that these

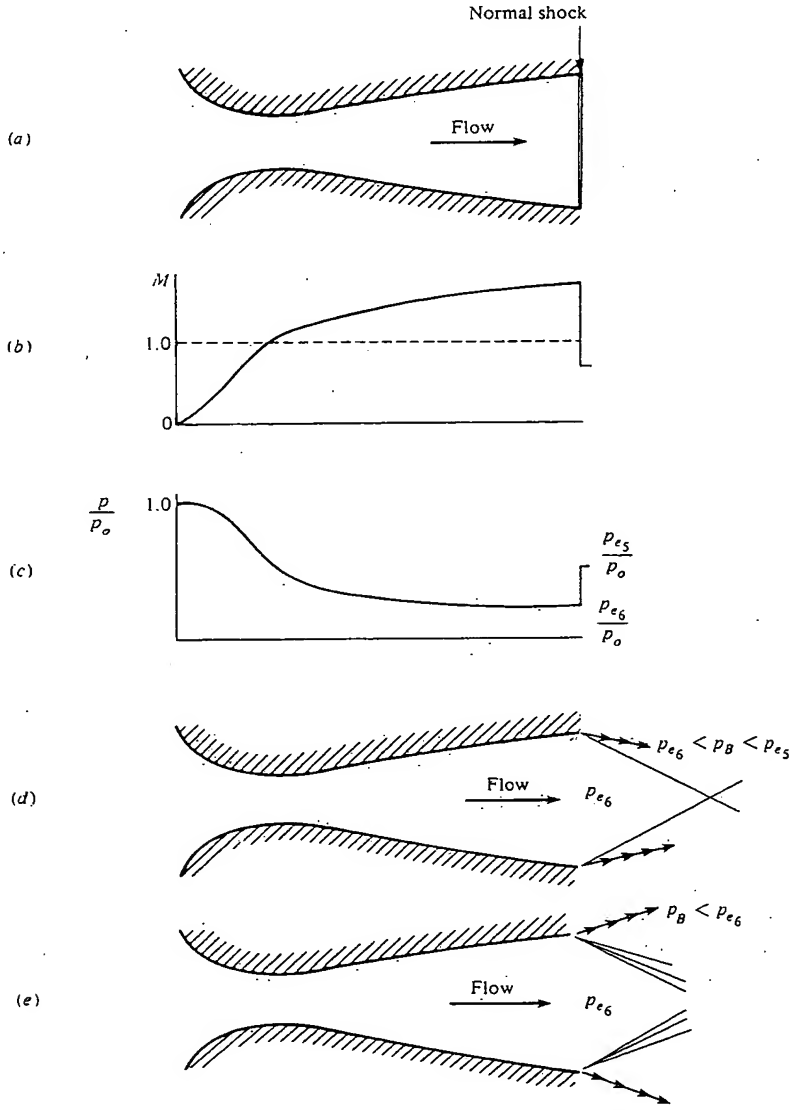

FIGURE 5.13
Flow with shock and expansion waves at the exit of a convergent-divergent nozzle.

quasi-one-dimensional considerations allow the analysis of cross-sectional averaged properties inside a nozzle of given shape. They do not tell us much about how to design the *contour* of a nozzle—especially that for a supersonic nozzle in order to ensure shockfree, isentropic flow. If the shape of the walls of a supersonic nozzle is not just right, oblique shock waves can occur inside the nozzle. The proper contour for a supersonic nozzle can be determined from the method of characteristics, to be discussed in Chap. 11.

Example 5.1. Consider the subsonic-supersonic flow through a convergent-divergent nozzle. The reservoir pressure and temperature are 10 atm and 300 K, respectively. There are two locations in the nozzle where $A/A^* = 6$: one in the convergent section and the other in the divergent section. At each location, calculate M, p, T, and u.

Solution. In the *convergent* section, the flow is subsonic. From the front of Table A.1, for subsonic flow with $A/A^* = 6$: $\boxed{M = 0.097}$, $p_o/p = 1.006$, and $T_o/T = 1.002$. Hence

$$p = \frac{p}{p_o} p_o = (1.006)^{-1}(10) = \boxed{9.94 \text{ atm}}$$

$$T = \frac{T}{T_o} T_o = (1.002)^{-1}(300) = \boxed{299.4 \text{ K}}$$

$$a = \sqrt{\gamma RT} = \sqrt{(1.4)(287)(299.4)} = 346.8 \text{ m/s}$$

$$u = Ma = (0.097)(346.8) = \boxed{33.6 \text{ m/s}}$$

In the *divergent* section, the flow is supersonic. From the supersonic section of Table A.1, for $A/A^* = 6$: $\boxed{M = 3.368}$, $p_o/p = 63.13$, and $T_o/T = 3.269$. Hence

$$p = \frac{p}{p_o} p_o = (63.13)^{-1}(10) = \boxed{0.1584 \text{ atm}}$$

$$T = \frac{T}{T_o} T_o = (3.269)^{-1}(300) = \boxed{91.77 \text{ K}}$$

$$a = \sqrt{\gamma RT} = \sqrt{(1.4)(287)(91.77)} = 192.0 \text{ m/s}$$

$$u = Ma = (3.368)(192.0) = \boxed{646.7 \text{ m/s}}$$

Example 5.2. A supersonic wind tunnel is designed to produce Mach 2.5 flow in the test section with standard sea level conditions. Calculate the exit area ratio and reservoir conditions necessary to achieve these design conditions.

Solution. From Table A.1, for $M_e = 2.5$:

$$\boxed{A_e/A^* = 2.637} \qquad p_o/p_e = 17.09 \qquad T_o/T_e = 2.25$$

Also, at standard sea level conditions, $p_e = 1$ atm and $T_e = 288$ K. Hence,

$$p_o = \frac{p_o}{p_e} p_e = (17.09)(1) = \boxed{17.09 \text{ atm}}$$

$$T_o = \frac{T_o}{T_e} T_e = (2.25)(288) = \boxed{648 \text{ K}}$$

Example 5.3. Consider a rocket engine burning hydrogen and oxygen; the combustion chamber temperature and pressure are 3571 K and 25 atm, respectively. The molecular weight of the chemically reacting gas in the combustion chamber is 16, and $\gamma = 1.22$. The pressure at the exit of the convergent-divergent rocket nozzle is 1.174×10^2 atm. The area of the throat is 0.4 m^2. Assuming a calorically perfect gas, calculate: (a) the exit Mach number, (b) the exit velocity, (c) the mass flow through the nozzle, and (d) the area of the exit.

Solution. Note that for this problem, where $\gamma = 1.22$, the compressible flow tables in the Appendix *cannot* be used since the tables are calculated for $\gamma = 1.4$. Thus, to solve this problem, we have to use the governing equations directly.

(a) To obtain the exit Mach number, use the isentropic relation given by Eq. (3.30):

$$\frac{p_o}{p_e} = \left(1 + \frac{\gamma - 1}{2} M_e\right)^{\gamma/(\gamma-1)}$$

or

$$M_e^2 = \frac{2}{\gamma - 1}\left[\left(\frac{p_o}{p_e}\right)^{(\gamma-1)/\gamma} - 1\right] = \frac{2}{0.22}\left[\left(\frac{25}{1.174 \times 10^{-2}}\right)^{0.22/1.22} - 1\right] = 27.116$$

$$\boxed{M_e = 5.21}$$

To obtain the exit velocity:

(b)

$$\frac{T_e}{T_o} = \left(\frac{p_e}{p_o}\right)^{(\gamma-1)/\gamma} = \left(\frac{1.174 \times 10^{-2}}{25}\right)^{0.180} = 0.02517$$

$$T_e = 0.02517 T_o = 0.02517(35617) = 885.3 \text{ K}$$

From Sec. 1.4, we know that

$$R = \frac{\mathscr{R}}{\mathscr{M}} = \frac{8314}{16} = 519.6 \text{ J/kg} \cdot \text{K}$$

$$a_e = \sqrt{\gamma R T_e} = \sqrt{(1.22)(519.6)(885.3)} = 749.1 \text{ m/s}$$

$$V_e = M_e a_e = (5.21)(749.1) = \boxed{3903 \text{ m/s}}$$

(c) Since we are given $A^* = 0.4$ m^2, let us calculate the mass flow at the throat. First, obtain ρ_o from the equation of state:

$$\rho_o = \frac{p_o}{R T_o} = \frac{(25)(1.01 \times 10^5)}{(519.6)(3517)} = 1.382 \text{ kg/m}^3$$

CHAPTER 11 - RELEVANT CHAPTER

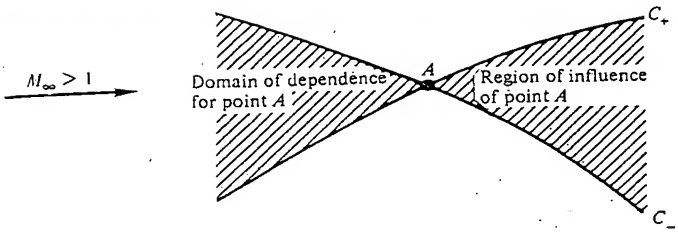

FIGURE 11.10
Domain of dependence and region of influence.

The above simple picture leads to the definition of two zones associated with point A, as illustrated in Fig. 11.10. Consider the left- and right-running characteristics through point A. The area between the two upstream characteristics is defined as the *domain of dependence* for point A. Properties at point A "depend" on any disturbances or information in the flow within this upstream region. The area between the two downstream characteristics is defined as the *region of influence* of point A. This region is "influenced" by any action that is going on at point A. Clearly, disturbances that are generated at point A do *not* propagate upstream. This is a general and important behavior of steady supersonic flow—*disturbances do not propagate upstream*. (However, keep in mind from Chap. 7 that, in an *unsteady* supersonic flow, compression waves can propagate upstream.)

11.7 SUPERSONIC NOZZLE DESIGN

In order to expand an internal steady flow through a duct from subsonic to supersonic speed, we established in Chap. 5 that the duct has to be convergent-divergent in shape, as sketched in Fig. 11.11*a*. Moreover, we developed relations for the local Mach number, and hence the pressure, density, and temperature, as functions of local area ratio A/A^*. However, these relations assumed quasi-one-dimensional flow, whereas, strictly speaking, the flow in Fig. 11.11*a* is two-dimensional. Moreover, the quasi-one-dimensional theory tells us nothing about the proper *contour* of the duct, i.e., what is the proper variation of area with respect to the flow direction $A = A(x)$. If the nozzle contour is not proper, shock waves may occur inside the duct.

The method of characteristics provides a technique for properly designing the contour of a supersonic nozzle for shockfree, isentropic flow, taking into account the multidimensional flow inside the duct. The purpose of this section is to illustrate such an application.

The subsonic flow in the convergent portion of the duct in Fig. 11.11*a* is accelerated to sonic speed in the throat region. In general, because of the

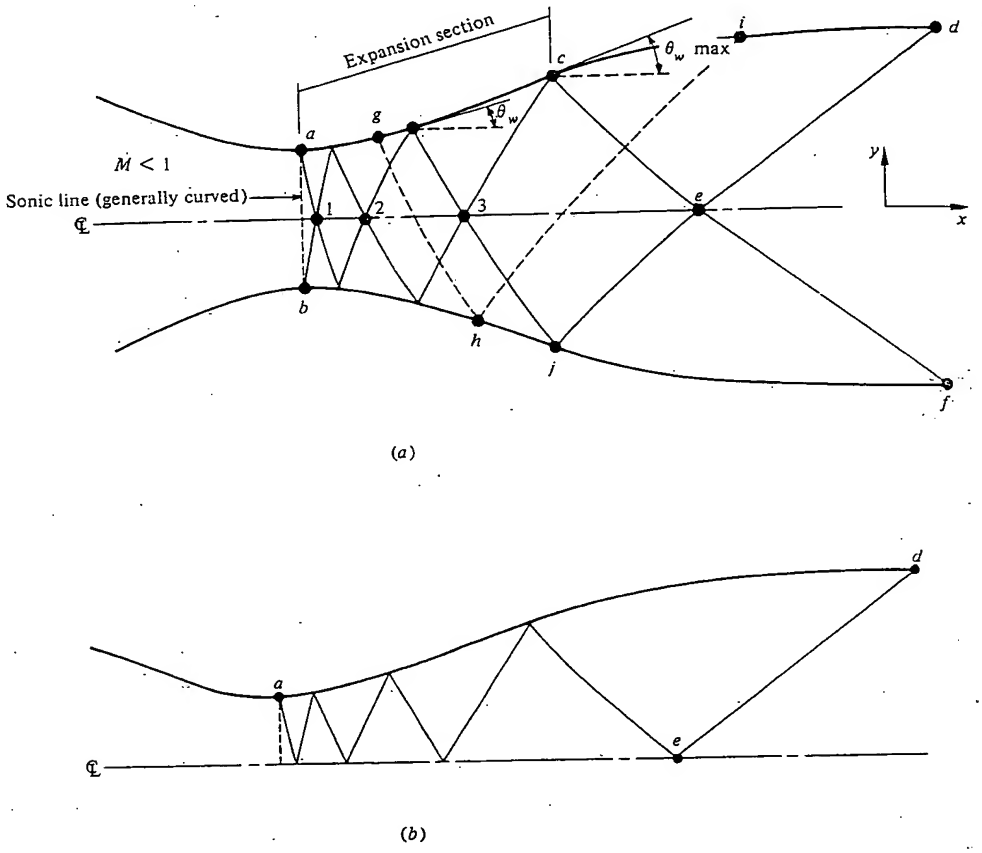

FIGURE 11.11
Schematic of supersonic nozzle design by the method of characteristics.

multidimensionality of the converging subsonic flow, the sonic line is gently curved. However, for most applications, we can assume the sonic line to be straight, as illustrated by the straight dashed line from a to b in Fig. 11.11a. Downstream of the sonic line, the duct diverges. Let θ_w represent the angle of the duct wall with respect to the x direction. The section of the nozzle where θ_w is increasing is called the *expansion* section; here, expansion waves are generated and propagate across the flow downstream, reflecting from the opposite wall. Point c is an inflection point of the contour, where $\theta_w = \theta_{w_{max}}$. Downstream of point c, θ_w decreases until the wall becomes parallel to the x direction at points d and f. The section from c to d is a "straightening" section specifically designed to cancel all the expansion waves generated by the expansion section. For

example, as shown by the dashed line in Fig. 11.11*a*, the expansion wave generated at *g* and reflected at *h* is cancelled at *i*. Also shown in Fig. 11.11*a* are the characteristic lines going through points *d* and *f* at the nozzle exit. These characteristics represent infinitesimal expansion waves in the nozzle, i.e., Mach waves. Tracing these two characteristics upstream, we observe multiple reflections up to the throat region. The area *acejb* is the expansion region of the nozzle, covered with both left- and right-running characteristics. Such a region with waves of both families is defined as a *nonsimple region* (analogous to the nonsimple waves described for unsteady one-dimensional flow in Sec. 7.7). In this region, the characteristics are curved lines. In contrast, the regions *cde* and *jef* are covered by waves of only one family because the other family is cancelled at the wall. Hence, these are *simple regions*, where the characteristic lines are straight. Downstream of *def*, the flow is uniform and parallel, at the desired Mach number. Finally, due to the symmetry of the nozzle flow, the waves (characteristics) generated from the top wall act as if they are "reflected" from the centerline. This geometric ploy due to symmetry allows us to consider in our calculations only the flow above the centerline, as sketched in Fig. 11.11*b*.

Supersonic nozzles with gently curved expansion sections as sketched in Fig. 11.11*a* and *b* are characteristic of wind tunnel nozzles where high-quality, uniform flow is desired in the test section (downstream of *def*). Hence, wind tunnel nozzles are long, with a relatively slow expansion. By comparison, rocket nozzles are short in order to minimize weight. Also, in cases where rapid expansions are desirable, such as the nonequilibrium flow in modern gasdynamic lasers (see Ref. 21), the nozzle length is as short as possible. In such *minimum-length nozzles*, the expansion section in Fig. 11.11*a* is shrunk to a point, and the expansion takes place through a centered Prandtl-Meyer wave emanating from a sharp-corner throat with an angle θ_{w_{max}, M_L}, as sketched in Fig. 11.12*a*. The length of the supersonic nozzle, denoted as L in Fig. 11.12*a* is the minimum value consistent with shockfree, isentropic flow. If the contour is made shorter than L, shocks will develop inside the nozzle.

Assume that the nozzles sketched in Figs. 11.11*a* and 11.12*a* are designed for the same exit Mach numbers. For the nozzle in Fig. 11.11a with an arbitrary expansion contour *ac*, multiple reflections of the characteristics (expansion waves) occur from the wall along *ac*. A fluid element moving along a streamline is constantly accelerated while passing through these multiple reflected waves. In contrast, for the minimum-length nozzle shown in Fig. 11.12*a*, the expansion contour is replaced by a sharp corner at point *a*. There are no multiple reflections and a fluid element encounters only two systems of waves—the right-running waves emanating from point *a* and the left-running waves emanating from point *d*. As a result, θ_{w_{max}, M_L} in Fig. 11.12*a* must be larger than $\theta_{w_{max}}$ in Fig. 11.11*a*, although the exit Mach numbers are the same.

Let ν_M be the Prandtl-Meyer function associated with the design exit Mach number. Hence, along the C_+ characteristic *cb* in Fig. 11.12*a*, $\nu = \nu_M = \nu_c = \nu_b$. Now consider the C_- characteristic through points *a* and *c*. At point *c*, from

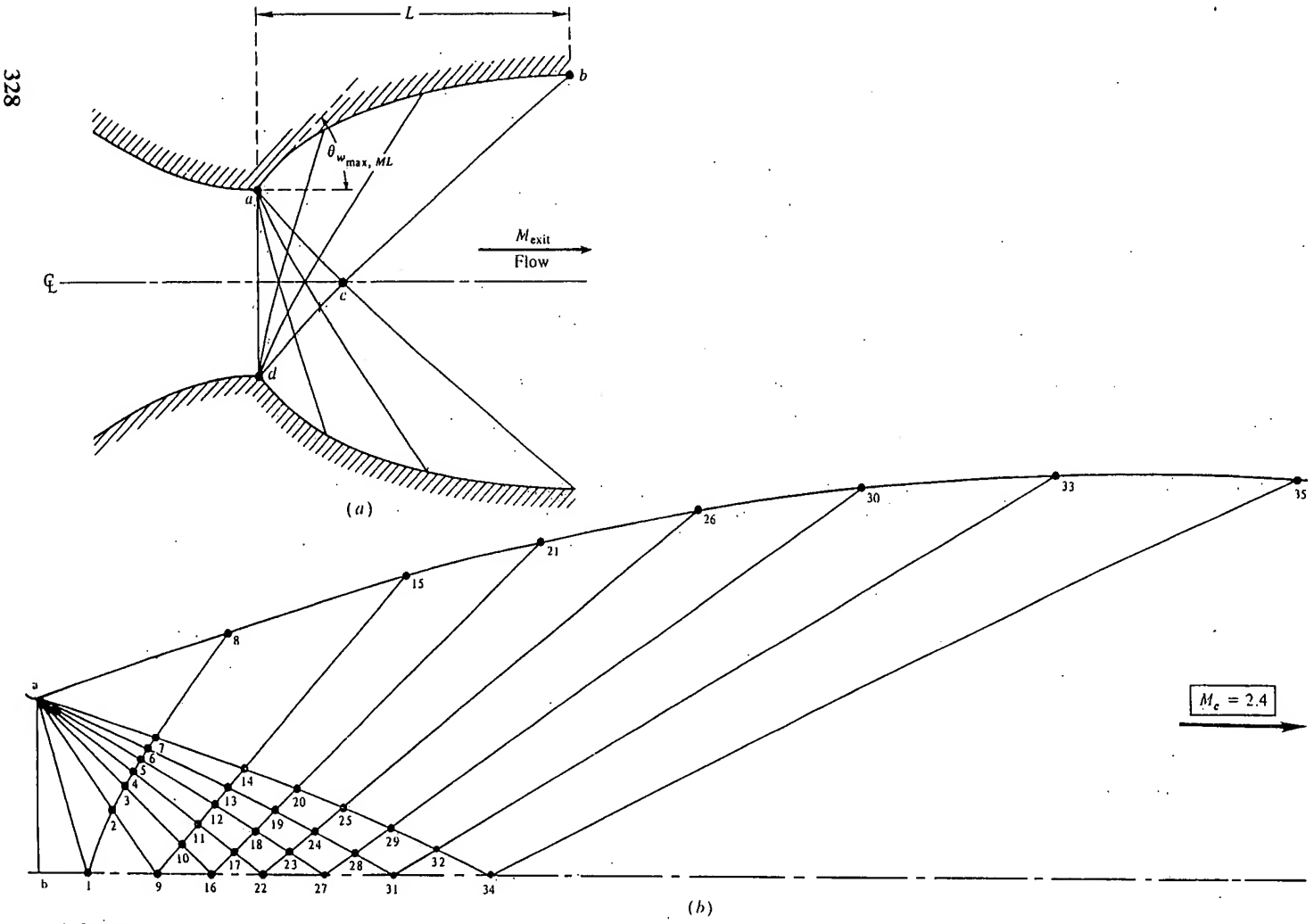

FIGURE 11.12
(*a*) Schematic of minimum-length nozzle. (*b*) Graphical construction for Example 11.1.

Eq. (11.20),

$$\theta_c + \nu_c = (K_-)_c \tag{11.28}$$

However, $\theta_c = 0$ and $\nu_c = \nu_M$. Hence, from Eq. (11.28),

$$(K_-)_c = \nu_M \tag{11.29}$$

At point a, along the same C_- characteristic ac, from Eq. (11.20),

$$\theta_{w_{max},\, M_L} + \nu_a = (K_-)_a \tag{11.30}$$

Since the expansion at point a is a Prandtl-Meyer expansion from initially sonic conditions, we know from Sec. 4.13 that $\nu_a = \theta_{w_{max},\, M_L}$. Hence, Eq. (11.30) becomes

$$\theta_{w_{max},\, M_L} = \tfrac{1}{2}(K_-)_a \tag{11.31}$$

However, along the same C_- characteristic, $(K_-)_a = (K_-)_c$; hence Eq. (11.31) becomes

$$\theta_{w_{max},\, M_L} = \tfrac{1}{2}(K_-)_c \tag{11.32}$$

Combining Eqs. (11.29) and (11.32), we have

$$\boxed{\theta_{w_{max},\, M_L} = \frac{\nu_M}{2}} \tag{11.33}$$

Equation (11.33) demonstrates that, *for a minimum-length nozzle the expansion angle of the wall downstream of the throat is equal to one-half the Prandtl-Meyer function for the design exit Mach number*. For other nozzles such as that sketched in Fig. 11.11*a*, the maximum expansion angle is *less* than $\nu_M/2$.

The shape of the finite-length expansion section in Fig. 11.11*a* can be somewhat arbitrary (within reason). It is frequently taken to be a circular arc with a diameter larger than the nozzle throat height. However, once the shape of the expansion section is chosen, then its length and $\theta_{w_{max}}$ are determined by the design exit Mach number. These properties can be easily found by noting that the characteristic line from the end of the expansion section intersects the centerline at point e, where the local Mach number is the same as the design exit Mach number. Hence, to find the expansion section length and $\theta_{w_{max}}$, simply keep track of the centerline Mach number (at points 1, 2, 3, etc.) as you construct your characteristics solution starting from the throat region. When the centerline Mach number equals the design exit Mach number, this is point e. Then the expansion section is terminated at point c, which fixes both its length and the value of $\theta_{w_{max}}$.

Example 11.1. Compute and graph the contour of a two-dimensional minimum-length nozzle for the expansion of air to a design exit Mach number of 2.4.

Solution. The results of this problem are given in Fig. 11.12*b*. To begin with, the sonic line at the throat, ab, is assumed to be straight. The first characteristic ($a - 1$)

emanating from the sharp throat is chosen as inclined only slightly from the normal sonic line. ($\Delta\theta = 0.375°$; hence $\theta + \nu = 0.75°$ and $dy/dx = \theta - \mu = -73.725°$.) The remainder of the expansion fan is divided into six increments with $\Delta\theta = 3°$. The total corner angle $\theta_{w_{max}} = \nu/2 = 36.75°/2 = 18.375°$. The values of K_+, K_-, θ, and ν are tabulated in Table 11.1 for all grid points. The nozzle contour is drawn by starting at the throat corner (where $\theta_a = \theta_{w_{max}} = 18.375°$), drawing a straight line with an average slope, $\frac{1}{2}(\theta_a + \theta_8)$, and defining point 8 on the contour as the intersection of this straight line with the left-running characteristic 7-8. Point 15 is located by the intersection of a straight line through point 8 having a slope of $\frac{1}{2}(\theta_8 + \theta_{15})$ with the left-running characteristic 14-15. This process is repeated to generate the remainder of the contour, points 21, 26, etc.

For this example, the computed area ratio $A_e/A^* = 2.33$. This is within 3 percent of the value $A_e/A^* = 2.403$ from Table A.1. This small error is induced by the graphical construction of Fig. 11.12*b*, and by the fact that only seven increments are chosen for the corner expansion fan. For a more accurate calculation, finer increments should be used, resulting in a more closely spaced characteristic net throughout the nozzle.

Note that a small inconsistency is involved with the properties at point 1 in Fig. 11.12, as listed in the first line of Table 11.1. The entry in Table 11.1 for θ at point 1 is a nonzero (but small) number, namely 0.375°. This is inconsistent with the physical picture in Fig. 11.12, which shows point 1 on the nozzle centerline where $\theta = 0$. This inconsistency is due to the necessity of *starting* the calculations with the straight characteristic line, a-1, along which the value of θ is constant and equal to 0.375°. In reality, the characteristic a-1 is curved because of the nonuniform flow inside the region a-b-1 in Fig. 11.12, but we have no way of knowing what that nonuniform flow is for this problem. In Sec. 12.7, we will show that a finite-difference calculation in the throat region can provide such information. However, within the framework of the method of characteristics in the present section, we must live with this inconsistency. As long as the first characteristic line a-1 is taken as close as possible to the assumed straight sonic line, this inconsistency will be minimized.

11.8 METHOD OF CHARACTERISTICS FOR AXISYMMETRIC IRROTATIONAL FLOW

For axisymmetric irrotational flow, the philosophy of the method of characteristics is the same as discussed earlier; however, some of the details are different, principally the compatibility equations. The purpose of this section is to illustrate those differences.

Consider a cylindrical coordinate system as sketched in Fig. 11.13. The cylindrical coordinates are r, ϕ, and x, with corresponding velocity components v, w, and u, respectively. In these cylindrical coordinates, the continuity equation

$$\nabla \cdot (\rho \mathbf{V}) = 0$$